Front. Phys. China (2006) 2:143–159
DOI 10.1007/s 11467-006-0004-1

REVIEW ARTICLE

ZHI Qi-jun, Mao Ying-chen, REN Zhong-zhou

Macroscopic-microscopic calculations of ground state properties of superheavy nuclei

Abstract We systematically calculate the ground state properties of superheavy even-even nuclei with proton number Z=94−118. The calculations are based on the liquid drop macroscopic model and the microscopic model with the modified single-particle oscillator potential. The calculated binding energies and α-decay energies agree well with the experimental data. The reliability of the macroscopic-microscopic(MM)model for superheavy nuclei is confirmed by the good agreement between calculated results and experimental ones. Detailed comparisons between our calculations and Möller's are made. It is found that the calculated results also agree with Möller's results and that the MM model is insensitive to the microscopic single-particle potential. Calculated results are also compared with results from relativistic mean-field (RMF) model and from Skyrme-Hatree-Fock(SHF) model. In addition, half-lives, deformations and shape coexistence are also investigated. The properties of some unknown nuclei are predicted and they will be useful for future experimental researches of superheavy nuclei.

Keywords superheavy nuclei, macroscopic-microscopic model, groundstate properties

PACS numbers 27.90.+b, 21.10.Dr, 21.10.Tg

ZHI Qi-jun, MAO Ying-chen, REN Zhong-zhou(✉)
Department of Physics, Nanjing University, Nanjing 210008, China

REN Zhong-zhou
Center of Theoretical Nuclear Physics,
National Laboratory of Heavy-Ion Accelerator,
Lanzhou 730000, China

REN Zhong-zhou
CPNPC, Nanjing University,
Nanjing 210008, China
E-mail: zren@nju.edu.cn

Received March 22,2006

1 Introduction

Studies of superheavy elements are current interests in nuclear physics. In recent years, with the rapid development of modern accelerators, many new superheavy elements have been synthesized [1–11]. During 1995–1996, the elements Z=110–112 were produced by Hofmann *et al.* at GSI in Germany [1–3]. In 1999, the element Z=114 was produced by Oganessian *et al.* at Dubna in Russia [6, 7]. In 2000, the element Z=116 was synthesized at Dubna [8]. The element Z=110 was confirmed in 2002 by the Lawrence Berkeley National Laboratory in USA [9] and by the Institute of Physical and Chemical Research (RIKEN) in Japan [10]. The confirmation of Z=111 was made at Lawrence Berkeley National Laboratory [11] and at RIKEN in 2004. At present, many large laboratories participate in this field and some interesting results such as α-decay energies and half-lives were reported very recently[12–18]. These new experimental data will promote both theoretical and experimental researches of superheavy nuclei.

Theoretical calculation is very important for the proposal of the new experiment with the aim of producing new superheavy nuclei. Some theoretical efforts have been made in the past years [19–29]. However, the theoretical model that was used is founded in the β-stability line, so the reliability and applicability of these models still need to be verified when it is used in superheavy nuclei. The self-consistent mean-field model has been widely used in the studies of nuclei [19–27]. The properties of superheavy nuclei on the decay chain of Z=110–112 and Z=114 in the framework of RMF model has been systematically calculated [22, 23]. Shape coexistence is predicted in the ground state of superheavy nuclei and deformation can be an important cause for the stability of superheavy nuclei based on a constraint RMF calculations [22,23]. The shape coexistence of superheavy nuclei in Refs. [22,23] is also supported by Skyrme-Hartree-Fock calculations [26,28,29]. The reliability of the RMF model has been verified when it

is used to study the superheavy nuclei [24,25]. Besides the self-consistent approaches and relativistic mean field method, the macroscopic-microscopic (MM) approach, which grafts the microscopic corrections onto the macroscopic model, is often used to study the properties of nuclei [30–35]. Myers and Swiatecki successfully produced the known magic number and predicted the islands of stability by this model [33]. Möller *et al.* systematically calculated the nuclear ground state properties by this model [30, 31]. In the framework of macroscopic-microscopic model, there are many calculations based on folded Yukawa single-particle potential or Woods-Saxon single-particle potential [30–32, 35]. It is interesting to see whether the results obtained from the MM model are sensitive to the effective single-particle potential (microscopic model) and the macroscopic model used in the calculation. To that end, in this paper, we use the modified single-particle oscillator potential as the microscopic single-particle potential and the liquid drop model to study the properties of superheavy nuclei. It is well known that the cranked Nilsson model, where the modified single-particle oscillator potential was adopted, has been successfully used in the description of high-spin state and deformation state [36–39]. We expect that the MM model, where the modified single-particle oscillator potential is adopted as the microscopic single-particle potential, can also be used to study the properties of superheavy nuclei. Based on this point, we systematically calculate the ground state properties of superheavy nuclei with proton number Z=94–118 within the framework of the MM model. The calculations include binding energies, α-decay energies, shape parameters and half-lives. Comparisons between calculated results and experimental data are made to test the reliability of this model. Detailed comparisons with Möller's calculations are also made. We think these comparisons are necessary for testing the reliability and stability of MM model. In addition, the predicted properties of some unknown nuclei are useful for future experimental research in superheavy nuclei.

This paper is organized in the following way. Section 2 contains the main formalism of the MM model. The numerical results and detailed discussions are given in Sec tion 3. Section 4 is a short summary of this work.

2 The formalism of the macroscopic-microscopic model

In the macroscopic-microscopic approach, the total potential energy is the sum of a macroscopic term and a microscopic term representing the shell plus pairing correction. It can be written as:

$$E_{\rm tot} = E_{\rm mac}(Z,N,\vec{\varepsilon}) + E_{\rm mic}(Z,N,\vec{\varepsilon}) \tag{1}$$

where $E_{\rm mic}$ is :

$$E_{\rm mic} = E_{\rm shell}(Z,N,\vec{\varepsilon}) + E_{\rm pair}(Z,N,\vec{\varepsilon}) \tag{2}$$

Detailed information about the macroscopic-microscop ic model can be found in Refs.[30,31]. There are several different models for the macroscopic term, such as liquid-drop model, droplet model, finite-range drop model and so on [30, 31, 33, 34, 40]. It is well known that the liquid drop model (LDM) is successful in reproducing the nuclear mass [40]. As pointed out by Ragnarsson [39], the LDM can be reliably used to study nuclear deformations and high spin states, although it gives somewhat too high fission barriers for some isotopes. In this paper, because we are mainly interested in the properties of ground state and do not want to calculate the fission barriers, we prefer the LDM model [33] to other complicated models, which involve more formulas, as the macroscopic model. In this model, the macroscopic energy is given by:

$$\begin{aligned} E_{LD} = & -a_\upsilon\left(1-K_\upsilon\left(\frac{N-Z}{A}\right)^2\right)A \\ & +\frac{3}{5}\frac{e^2Z^2}{R_c}\left(B_c(\vec{\varepsilon})-\frac{5\pi^2}{6}\left(\frac{d}{R_c}\right)^2\right) \\ & +a_S\left(1-K_S\left(\frac{N-Z}{A}\right)^2\right)A^{2/3}B_s(\vec{\varepsilon}) \\ & \begin{cases} +12/\sqrt{A}, & \text{odd-odd nuclei} \\ 0, & \text{odd-even nuclei} \\ -12/\sqrt{A}, & \text{even-even nuclei} \end{cases} \end{aligned} \tag{3}$$

where $\vec{\varepsilon}=(\varepsilon_2,\gamma,\varepsilon_4)$, and $\varepsilon_2,\gamma,\varepsilon_4$ are the quadrupole and hexadecapole deformation degrees of freedom. The liquid-drop parameters are chosen as follows according to that in Myers and Swiatecki [33]:

$$a_\upsilon = 15.494\,1\ \text{MeV},\ a_S = 17.943\,9\ \text{MeV}$$

$$K_\upsilon = K_S = 1.782\,6,\ d = 0.546\ \text{fm},\ R_c = 1.224\,9A^{1/3}\text{fm}$$

There exist several different single-particle potentials for the microscopic term. Möller *et al.* systematically studied the nuclear properties with the folded-Yukawa single-particle potential [30, 31]. Considering that all matrix elements can be given in analytic form with modified oscillator potential and that the cranked Nilsson model has been successfully used in high-spin state and deformed state, we adopt the modified single-particle oscillator potential as the microscopic potential in this paper. Because we are interested in the ground state properties, we consider ε_2 and ε_4 deformation and neglect the ε_6 deformation and other multipole deformation in this paper. The modified single-particle oscillator potential used here is of the form [41]:

$$h = h_{ho}(\varepsilon_2,\gamma) + 2\hbar\omega_0\rho^2\sqrt{\frac{4\pi}{9}}\omega_4 V_4(\gamma) + V' - \omega j_x \tag{4}$$

Because the nuclear spin of ground state is zero for even-even nuclei, we neglect the last term ωj_x in our calculation. The term $h_{ho}(\varepsilon_2,\gamma)$ is the anisotropic harmonic oscillator potential

$$h_{ho}(\varepsilon,\gamma) = \frac{p^2}{2m} + \frac{1}{2}m(\omega_x^2x^2 + \omega_y^2y^2 + \omega_z^2z^2) \tag{5}$$

ω_x, ω_y, ω_z are expressed in quadrupole deformation

parameters, and more discussions can be found in Refs. [41, 42]. $V_4(\gamma)$ is the hexadecapole potential, it is of the form:

$$V_4 = a_{40}Y_4^0 + a_{42}(Y_4^2 + Y_4^{-2}) + a_{44}(Y_4^4 + Y_4^{-4}) \quad (6)$$

where a_{4i} are chosen as:

$$a_{40} = \frac{1}{6}(5\cos^2\gamma + 1),\ a_{42} = \frac{1}{12}\sqrt{30}\sin 2\gamma \quad (7)$$

$$a_{44} = \frac{1}{12}\sqrt{70}\sin^2\gamma \quad (8)$$

The term V' is introduced to reproduce the level sequence as observed in nuclei. It is of the form:

$$V' = -\kappa(N)\hbar\overset{o}{\omega}_0\left\{2l_t\cdot s + \mu(N)\left(l_t^2 - \left\langle l_t^2\right\rangle_N\right)\right\} \quad (9)$$

the oscillator strength $\overset{o}{\omega}_0$ is chosen as

$$\hbar\overset{o}{\omega}_{0\mathrm{p/n}} = \frac{41}{A^{1/3}}\left(1 \mp \frac{N-Z}{3A}\right)\ \text{(MeV)} \quad (10)$$

for protons and neutrons respectively. The parameters κ and μ are dependent on the main oscillator quantum number.

After all parameters are determined, the diagonalization of Hamiltonian (4) gives the eigenvalues that can be used for the calculation of shell correction and pairing correction. Here we use Strutinsky's shell correction method to calculate the shell energy:

$$E_{\mathrm{shell}} = E_{sp} - \tilde{E}_{\mathrm{sp}} \quad (11)$$

where E_{sp} is the total single-particle energy, $\tilde{E}_{sp}$ is the smoothed total single-particle energy.

$$\tilde{E}_{sp} = \int_{-\infty}^{\varepsilon_f}\varepsilon\tilde{g}(\varepsilon)\mathrm{d}\varepsilon \quad (12)$$

and

$$\tilde{g}(\varepsilon) = \frac{1}{\gamma\sqrt{\pi}}\sum_i n_i \exp\{-(\varepsilon-\varepsilon_i)^2/\gamma^2\} \quad (13)$$

Detailed information about shell correction is discussed in Refs. [41, 43, 44]. The pairing energy is calculated by the BCS model. The pairing strength is chosen as:

$$G_{\mathrm{p,n}} = \frac{1}{A}\left(g_0 \pm g_1\frac{N-Z}{A}\right)\ \text{(MeV)} \quad (14)$$

for protons and neutrons respectively, and g_0=19.2, g_1=7.4. More discussions about BCS pairing calculation can be found in Refs. [41, 42].

The ground state should have the lowest energy. Therefore, it can be obtained by minimizing the energy with respect to shape parameters $\varepsilon_2, \gamma, \varepsilon_4$ at each point. After the ground state is obtained, we can calculate the binding energies, α-decay energies, shape parameters, half-lives and so on. In our calculation we set γ=0, which means that an axial deformation is assumed in superheavy nuclei.

3 Numerical results and discussions

The values of κ, μ are important parameters in the Nilsson potential. There has been a great deal of discussions about the values in different masses regions [42, 45, 46]. Here we choose the standard parameters, which have been successfully used in the studies of high-spin states [36–38], according to the Lund systematics [41]. We do not make any adjustments on these parameters. The parameters are tabulated in Table 1. Using these parameters we systematically calculate the ground state properties of superheavy nuclei with proton number Z=94–118.

Table 1 (κ, μ) values as a function of the oscillator shell N for protons and neutrons.

N	κ_{p}	μ_{p}	κ_{n}	μ_{n}
0	0.120	0.00	0.120	0.00
1	0.120	0.00	0.120	0.00
2	0.105	0.00	0.105	0.00
3	0.090	0.30	0.090	0.25
4	0.065	0.57	0.070	0.39
5	0.060	0.65	0.062	0.43
6	0.054	0.69	0.062	0.34
7	0.054	0.69	0.062	0.26
8	0.054	0.69	0.062	0.26
9	0.054	0.69	0.062	0.26
10	0.054	0.69	0.062	0.26
11	0.054	0.69	0.062	0.26
12	0.054	0.69	0.062	0.26

3.1 Binding energies of superheavy nuclei

Binding energy is an important quantity of nuclei because it is directly related to the nuclear stability and α-decay energy. It is also an important input in the calculation of cross section in the research of superheavy nuclei. Using the MM model, we systematically calculate the binding energies (B), average binding energies (B/A), α-decay energies (Q_α),deformation parameters ($\varepsilon_2, \varepsilon_4$) for even-even nuclei on the isotopic chain of Z=94–118. In Table 2–6, we tabulate theoretical binding energy, quadrupole deformation, hexadecapole deformation, and α-decay energy, together with the available experimental data of the binding energy and α-decay energy. The theoretical binding energy, α-decay energy of Möller's calculation are also tabulated in these tables for comparison.

At first let us focus on the global behavior of the calculated binding energies. The MM results of Pu and Cm (Z=94, 96) isotopes are listed in Table 2. In Table 2, the first column is for nuclei, and columns 2–5 correspond to calculated results. The symbol ε_2 denotes the quadrupole deformation, ε_4 denotes the hexadecapole deformation, and B (MeV) is the theoretical binding energy. Further, the symbol Q_α (MeV) is the calculated α-decay energy.

Columns 6–7 correspond to theoretical binding energy and α-decay energy from by Möller's calculation [30]. The experimental binding energy and experimental α-decay

energy are listed in the last two columns of the table. They are obtained from the nuclear mass table [47, 48] and recent publications [4, 5, 15, 17, 18].

From Table 2, it is clearly seen that the calculated binding energies are very close to the experimental data. In the range of available experimental data, the average difference between theoretical binding energy and the experimental one is approximately 0.37 MeV. The maximum differences is about 0.6 MeV, and the relative difference is approximately 0.03%. Therefore one can say that the MM model reproduces the experimental binding energies. The modified single-particle oscillator potential can be reliably chosen as the microscopic single-particle potential for MM model to study the superheavy nuclei. This point is to be further confirmed in our following discussion.

Table 2 The binding energies, deformations and α-decay energies of even-even Pu and Cmisotopes. In row 1, Exp denotes experimental values (# for estimated values) [48] and Mol denotes Möller's results [30].

Nuclei	ε_2	ε_4	B /MeV	Q_α /MeV	B(Mol) /MeV	Q_α (Mol) /MeV	B(Exp) /MeV	Q_α (Exp) /MeV
^{232}Pu	0.182	–0.050	1 760.22	6.74	1 760.64	6.67	1760.6	6.71
^{234}Pu	0.190	–0.048	1 774.33	6.32	1 774.71	6.17	1774.8	6.31
^{236}Pu	0.197	–0.048	1 787.93	5.87	1 788.21	5.77	1788.5	5.87
^{238}Pu	0.206	–0.044	1 800.85	5.62	1 800.91	5.59	1801.4	5.59
^{240}Pu	0.208	–0.034	1 813.23	5.40	1 813.15	5.17	1813.6	5.26
^{242}Pu	0.215	–0.028	1 825.07	4.94	1 824.74	4.79	1825.2	4.98
^{244}Pu	0.220	–0.020	1 836.33	4.78	1 835.90	4.55	1836.3	4.67
^{246}Pu	0.218	–0.012	1 847.13	4.57	1 846.63	4.07	1846.7	4.35#
^{248}Pu	0.218	0.000	1 857.22	4.19	1 855.97	4.60		
^{250}Pu	0.212	0.002	1 866.92	3.88	1 864.92	4.24		
^{252}Pu	0.210	0.014	1 876.24	3.54	1 873.86	3.53		
^{254}Pu	0.200	0.014	1 885.14	3.22	1 882.65	2.91		
^{236}Cm	0.190	–0.045	1 781.36	7.15	1 781.82	7.12	1781.80#	7.10#
^{232}Cm	0.204	–0.038	1 795.79	6.84	1 796.19	6.82	1796.50	6.62
^{240}Cm	0.216	–0.035	1 809.62	6.61	1 809.98	6.52	1810.30	6.40
^{242}Cm	0.222	–0.035	1 822.93	6.16	1 823.05	6.16	1823.10	6.22
^{244}Cm	0.221	–0.027	1 835.71	5.75	1 835.79	5.65	1835.90	5.90
^{246}Cm	0.218	–0.020	1 847.76	5.65	1 847.86	5.18	1847.80	5.48
^{248}Cm	0.220	–0.010	1 859.21	5.50	1 859.28	4.92	1859.20	5.16
^{250}Cm	0.226	–0.003	1 870.21	5.10	1 869.39	5.53	1869.70	5.17
^{252}Cm	0.227	0.013	1 880.70	4.79	1 879.23	5.04	1879.80#	
^{254}Cm	0.215	0.015	1 890.74	4.48	1 888.77	4.44		
^{256}Cm	0.218	0.019	1 900.34	4.21	1 898.31	3.84		
^{258}Cm	0.209	0.024	1 909.50	3.94	1 907.49	3.45		

One can see that the binding energies of our calculation are in good agrement with those of Möller's through the comparison between the two sets of theoretical results. In the range where the experimental data are known, the maximum difference between our results and Möller's is less than 0.4 MeV. This surprising agreement between the two sets of theoretical results confirms the reliability of both calculations. In the unknown nuclei region, the two sets of theoretical binding energies are in good agrement too, and the maximum difference is less than 2.5 MeV. Because the total binding energy is around 1 900 MeV, the maximum relative difference is approximately 0.1%.

In order to see the systematic behavior of the agreement between the model and the experimental data, we draw the variation of the theoretical binding energies and experimental ones in Fig. 1. Figure 1 shows the variation of the average binding energy (B/A) with nucleon number for Pu, Cm, Cf, Fm, No, Rf, Sg, Hs (Z=94–108) isotopes. It can be divided into four parts. Figure 1(a) shows the results for Pu and Cm isotopes. Figure 1(b) shows the results for Cf and Fm isotopes. Fig. 1c are the results for No and Rf isotopes. Figure 1(d) shows the results for Sg and Hs isotopes. Theoretical average binding energies of Möller's are also drawn in Fig. 1. In Fig. 1, hollow triangle denotes our calculated results while hollow inverted triangle denotes Möller's results. The black points are for experimental average binding energy.

From Fig. 1, one can clearly see that our theoretical average binding energies are in good agrement with the experimental ones. The calculations reproduce the measured binding energies quite accurately. In the known nuclei range, both our and Möller's calculated results are in good agreement with the experimental ones. The difference of both two theoretical results is too small to see in this region. In heavier isotopes (neutron rich region), there is a little discrepancy between the two sets of theoretical binding energies. This discrepancy is systematic and also interesting. We think this discrepancy in some nuclei may be due to

slightly different dependence of isospin for both macroscopic and microscopic term in the MM model. However, for globe behavior, the calculated results agree very well with the experimental data and with Möller's calculation. So the MM model, where the modified single-particle oscillator potential is adopted as the microscopic single-particle potential, can be applied to superheavy nuclei. The calculations are reliable and the predicted binding energies can be used for future experimental research.

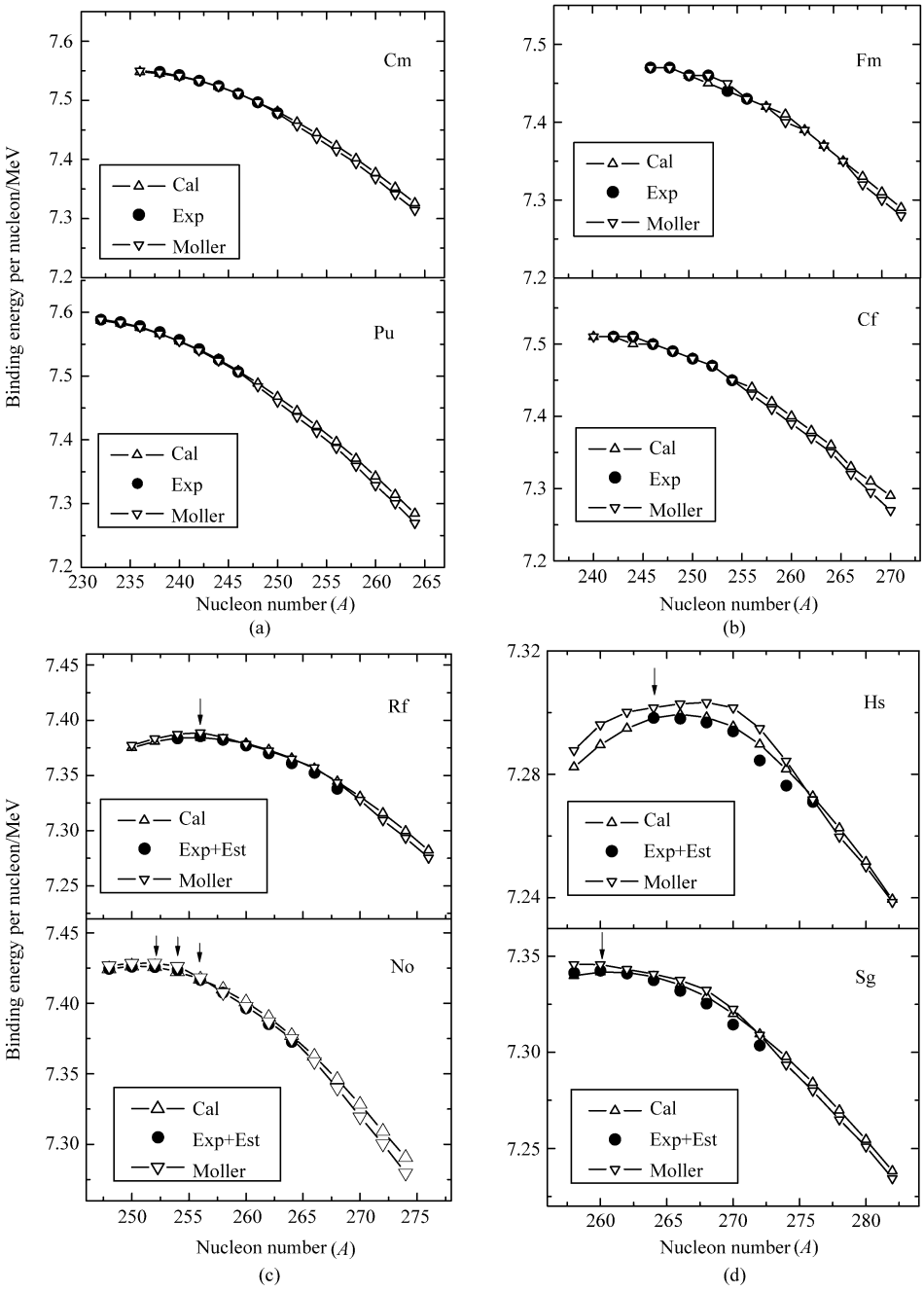

Fig. 1 The comparison of theoretical and experimental average binding energies (B/A) for Pu, Cm, Cf, Fm, No, Rf, Sg, and Hs isotopes. This includes all available data of binding energies on these isotopic chain. For Sg and Hs isotopes chain, the experimental and estimated binding energy of Audi [47] are denoted by black points. The experimental data of Sg and Hs are specially pointed out by a black arrow. It is interesting to note that both our theoretical and Möller's results agree with the experimental data well. The two sets of theoretical results agree with each other too.

In Table 3, we list the results for Cf and Fm isotopes. We use the same notations as those in Table 2. From Table 3, one can see that the theoretical binding energies of our calculations are very close to the experimental data. The relative difference between theoretical binding energies and experimental data is approximately 0.04%. The maximum

difference is 0.08%. This is rather a good theoretical model for calculation of binding energies. The good agreement between the theoretical results (columns 4 and 5 in Table 3) and experimental data (columns 8 and 9 in Table 3) is seen again. When we compare our results with Moller's results, the same conclusion as Table 2 can be reached. But in this range the difference between the two sets of theoretical results are smaller than that in Table 2. The maximum difference of binding energies is 1.7 MeV. From Fig. 1(b), one can clearly see that the two sets of theoretical results are also in good agreement with experimental data for Cf and Fm isotopes.

Table 3 Same as Table 2 but for even-even Cf and Fm isotopes .

Nuclei	ε_2	ε_4	B /MeV	Q_α /MeV	B(Mol) /MeV	Q_α (Mol) /MeV	B(Exp) /MeV	Q_α (Exp) /MeV
^{238}Cf	0.193	–0.043	1 786.63	7.98	1 787.12	7.95	1 787.10#	8.06#
^{240}Cf	0.208	–0.035	1 802.01	7.62	1 802.41	7.70	1 802.40#	7.72
^{242}Cf	0.218	–0.030	1 816.70	7.39	1 817.16	7.33	1 817.30	7.52
^{244}Cf	0.227	–0.020	1 830.83	7.09	1 831.38	6.90	1 831.30	7.33
^{246}Cf	0.230	–0.015	1 844.40	6.84	1 844.84	6.50	1 844.80	6.86
^{248}Cf	0.231	–0.013	1 857.37	6.65	1 857.82	6.27	1 857.80	6.36
^{250}Cf	0.235	–0.001	1 869.69	6.37	1 870.29	5.87	1 870.00	6.13
^{252}Cf	0.230	0.007	1 881.52	5.99	1 881.32	6.25	1 881.30	6.21
^{254}Cf	0.225	0.013	1 892.81	5.70	1 891.69	6.00	1 892.10	5.93
^{256}Cf	0.226	0.027	1 903.61	5.38	1 902.01	5.51	1 902.60#	5.56#
^{258}Cf	0.227	0.022	1 913.98	5.06	1 912.32	4.75		
^{260}Cf	0.213	0.027	1 923.89	4.75	1 922.28	4.33		
^{242}Fm	0.209	–0.033	1 806.30	8.64	1 806.99	8.43	1 806.60#	8.77#
^{244}Fm	0.229	–0.017	1 821.90	8.41	1 822.49	8.22	1 822.20#	8.55#
^{246}Fm	0.225	–0.020	1 836.94	8.05	1 837.63	7.82	1 837.20	8.38
^{248}Fm	0.234	–0.008	1 851.36	7.76	1 852.03	7.64	1 851.50	8.00
^{250}Fm	0.230	0.001	1 865.15	7.55	1 865.95	7.19	1 865.50	7.56
^{252}Fm	0.230	0.007	1 878.33	7.34	1 879.33	6.79	1 878.90	7.15
^{254}Fm	0.231	0.010	1 891.01	6.98	1 891.19	7.39	1 891.00	7.31
^{256}Fm	0.230	0.016	1 903.11	6.71	1 902.38	7.24	1 902.50	7.03
^{258}Fm	0.230	0.028	1 914.74	6.37	1 913.67	6.31	1 913.70#	6.66#
^{260}Fm	0.227	0.033	1 925.89	6.03	1 924.71	5.59	1 924.70#	6.18#
^{262}Fm	0.227	0.032	1 936.55	5.73	1 935.47	5.15		
^{264}Fm	0.221	0.033	1 946.63	5.56	1 945.16	5.42		

For nuclei with the proton number Z>100, the available experimental data of binding energies are very few. But for an overall test and detailed comparison between different calculations, we list both experimental binding energies and the the estimated values from Audi *et al.* [47] in Table 4, Table 5, and Table 6. The estimated values are denoted with symbol #. Theoretical binding energies and experimental results of No and Rf isotopes are shown in Table 4. Table 5 are for Sg and Hs isotopes. In Table 6, we tabulate theoretical results for Z=110 (D_s) and Z=112 isotopes. Previous discussions on Table 2 and Table 3 are also suitable for Table 4, Table 5, and Table 6. In these tables, the calculated binding energies are in good agreement with the experimental and estimated ones. The agreement between two sets of theoretical results is still nice. From Fig. 1(c),(d) one can clearly see that our results agree well with the experimental data and Möller's results.

After comparing the MM results of this article with the Moller model, we now compare the results of the MM model with those from the RMF model [25] and from Skyrme-Hatree-Fock (SHF) model [29]. The results are listed in Table 7 and drawn in Fig. 2. In our previous RMF research on superheavy nuclei [25], we set the upper limit and lower limit of binding energies by two sets of force parameters (TMA force and NL-Z2 force). This can be clearly seen in Table 7 and Fig. 2. It is found in Table 7 that our MM results are slightly closer to experimental data than those from other models. In Fig. 2, we draw the variation of different theoretical binding energies. It is obvious that the RMF results with TMA force set the upper limit of binding energies, while the ones with NL-Z2 force set the lower limit. The calculated results of MM model locate in the middle of the upper limit and lower limit, and give slightly better results. All of these results are useful for future experiments because the best one can be used as the prediction and the limits denote the uncertainty of theory from different models. In order to see the details of various model results, we calculate the root-mean-square (rms) deviation of binding energies for nuclei listed in Table 7. The root-mean-square deviation is:

$$(\Delta B)_{rms} = \sqrt{\frac{1}{n}\sum_{i=1}^{n}\left(B^i_{\exp} - B^i_{\text{the}}\right)^2} \qquad (15)$$

Table 4 Same as Table 2 but for even-even No and Rf isotopes.

Nuclei	ε_2	ε_4	B /MeV	Q_α /MeV	B(Mol) /MeV	Q_α (Mol) /MeV	B(Exp) /MeV	Q_α (Exp) /MeV
^{248}No	0.220	-0.015	1 841.27	8.93	1 841.82	8.97	1 841.24#	9.23#
^{250}No	0.230	-0.001	1 856.60	8.64	1 857.11	8.82	1 856.52#	8.95#
^{252}No	0.232	0.002	1 871.34	8.32	1 871.98	8.35	1 871.30	8.55
^{254}No	0.230	0.014	1 885.31	8.14	1 886.28	7.97	1 885.60	8.27
^{256}No	0.230	0.016	1 898.79	7.84	1 899.05	8.57	1 898.64	8.58
^{258}No	0.234	0.028	1 911.77	7.54	1 911.18	8.31	1 911.13#	8.15#
^{260}No	0.230	0.029	1 924.24	7.17	1 923.43	7.24	1 923.14#	7.70#
^{262}No	0.222	0.038	1 936.21	6.83	1 935.38	6.59	1 934.94#	7.10#
^{264}No	0.221	0.036	1 947.59	6.60	1 947.01	6.00	1 946.39#	6.58#
^{266}No	0.226	0.040	1 958.41	6.43	1 957.45	6.31		
^{268}No	0.220	0.034	1 968.73	6.20	1 967.11	6.34		
^{270}No	0.217	0.030	1 978.65	5.87	1 976.27	6.13		
^{254}Rf	0.230	0.013	1 875.49	9.42	1 876.38	9.03	1 875.44#	9.38#
^{256}Rf	0.231	0.016	1 890.39	9.26	1 891.53	8.75	1 890.67	8.93
^{258}Rf	0.239	0.022	1 904.68	8.93	1 905.25	9.32	1 904.64#	9.25#
^{260}Rf	0.230	0.028	1 918.52	8.57	1 918.39	8.96	1 918.04#	8.90#
^{262}Rf	0.234	0.034	1 931.81	8.26	1 931.54	7.93	1 930.94#	8.48#
^{264}Rf	0.229	0.046	1 944.50	8.05	1 944.40	7.32	1 943.29#	8.14#
^{266}Rf	0.216	0.052	1 956.80	7.65	1 956.95	6.73	1 955.74#	7.50#
^{268}Rf	0.211	0.046	1 968.28	7.60	1 968.14	7.16	1 966.59#	8.10#
^{270}Rf	0.207	0.043	1 979.32	7.39	1 978.45	7.29		
^{272}Rf	0.203	0.042	1 989.95	7.08	1 988.19	7.22		
^{274}Rf	0.201	0.038	2 000.12	6.83	1 998.38	6.19		
^{276}Rf	0.190	0.040	2 009.90	6.51	2 008.00	5.99		

Table 5 Same as Table 2 but for even-even Sg and Hs isotopes.

Nuclei	ε_2	ε_4	B /MeV	Q_α /MeV	B(Mol) /MeV	Q_α (Mol) /MeV	B(Exp) /MeV	Q_α (Exp) /MeV
^{258}Sg	0.237	0.017	1 893.69	10.10	1 895.22	9.45	1 894.1#	9.67#
^{260}Sg	0.233	0.024	1 908.86	9.82	1 909.90	9.93	1 909.04	9.92
^{262}Sg	0.229	0.036	1 923.51	9.48	1 923.94	9.61	1 923.34#	9.60#
^{264}Sg	0.227	0.043	1 937.62	9.20	1 937.98	8.70	1 937.13#	9.21#
^{266}Sg	0.229	0.047	1 951.15	8.95	1 951.82	8.02	1 950.35#	8.88
^{268}Sg	0.217	0.054	1 964.18	8.61	1 965.11	7.59	1 963.19#	8.40#
^{270}Sg	0.216	0.049	1 976.44	8.67	1 977.08	8.16	1 974.94#	9.10#
^{272}Sg	0.210	0.048	1 988.17	8.43	1 988.05	8.39	1 986.57#	8.30#
^{274}Sg	0.189	0.048	1 999.56	8.06	1 998.44	8.31		
^{276}Sg	0.184	0.049	2 010.45	7.80	2 009.29	7.20		
^{278}Sg	0.140	0.045	2 021.02	7.40	2 019.67	7.01		
^{280}Sg	0.134	0.044	2 031.28	6.92	2 030.27	6.03		
^{282}Sg	0.100	0.022	2 041.17	6.93	2 040.10	5.89		
^{264}Hs	0.228	0.036	1 926.75	10.41	1 927.62	10.57	1 926.74	10.59
^{266}Hs	0.231	0.047	1 941.64	10.17	1 942.55	9.69	1 941.29#	10.18
^{268}Hs	0.232	0.050	1 955.99	9.93	1 957.28	9.00	1 955.52#	9.90#
^{270}Hs	0.228	0.061	1 969.78	9.67	1 971.42	8.69	1 969.34#	9.30
^{272}Hs	0.226	0.059	1 982.79	9.70	1 984.20	9.20	1 981.38#	10.10#
^{274}Hs	0.196	0.056	1 995.19	9.55	1 995.91	9.46	1 993.73#	9.50#
^{276}Hs	0.172	0.050	2 007.30	9.17	2 007.03	9.32	2 006.80#	8.80#
^{278}Hs	0.160	0.045	2 018.99	8.86	2 018.21	8.53		
^{280}Hs	0.140	0.045	2 030.46	8.30	2 030.02	7.56		
^{282}Hs	0.124	0.044	2 041.53	7.79	2 041.29	6.68		
^{284}Hs	0.093	0.030	2 052.24	7.34	2 051.88	6.68		
^{286}Hs	-0.062	0.006	2 062.97	6.50	2 061.65	6.74		

Table 6 Same as Table 2 but for even-even Z=110 (D_s) and Z=112 (isotopes).

Nuclei	ε_2	ε_4	B /MeV	Q_α /MeV	B(Mol) /MeV	Q_α (Mol) /MeV	B(Exp) /MeV	Q_α (Exp) /MeV
^{268}110	0.227	0.043	1 943.78	11.27	1 944.97	10.94	1 943.12#	11.92#
^{270}110	0.217	0.050	1 958.91	11.02	1 960.53	10.31	1 958.40#	11.20
^{272}110	0.211	0.054	1 973.46	10.83	1 975.53	10.04	1 973.05#	10.76#
^{274}110	0.205	0.054	1 987.21	10.87	1 989.21	10.51	1 986.24#	11.40#
^{276}110	0.184	0.051	2 000.52	10.57	2 001.77	10.73	1 999.08#	10.60#
^{278}110	0.159	0.044	2 013.41	10.07	2 013.80	10.41	2 012.03#	10.00#
^{280}110	0.133	0.044	2 026.02	9.58	2 026.28	9.05	2 025.07#	9.30#
^{282}110	0.121	0.042	2 038.31	8.98	2 038.74	7.76		
^{284}110	0.101	0.037	2 050.20	8.56	2 050.75	7.57		
^{286}110	0.040	0.007	2 061.97	7.86	2 061.99	7.60		
^{288}110	-0.034	0.002	2 073.42	7.12	2 072.82	7.36		
^{272}112	0.211	0.044	1 960.08	12.00	1 961.66	11.61		
^{274}112	0.200	0.058	1 975.42	11.79	1 977.44	11.39		
^{276}112	0.187	0.048	1 989.97	11.79	1 991.99	11.84		
^{278}112	0.178	0.048	2 004.08	11.43	2 005.21	12.29	2 003.15#	11.38#
^{280}112	0.140	0.040	2 017.82	11.00	2 018.94	11.12	2 016.74#	10.62#
^{282}112	0.126	0.034	2 031.44	10.27	2 032.68	9.42	2 030.36#	9.96#
^{284}112	0.105	0.032	2 044.33	9.80	2 045.88	8.69	2 044.07#	9.30
^{286}112	-0.022	0.003	2 057.53	9.09	2 058.56	8.48		
^{288}112	0.001	-0.001	2 070.25	8.25	2 070.7	8.34		
^{290}112	0.003	0.001	2 082.44	7.83	2 082.64	7.64		

Table 7 The binding energies from our calculation, RMF [25], SHF [29], Möller *et al*. [30] and experiments [47].

Nuclei	The/MeV	TMA/MeV	Nl-Z2/MeV	SHF/MeV	Mol/MeV	Exp/MeV
^{234}Pu	1 774.3	1 775.2	1 773.8	1 773.9	1 774.7	1 774.8
^{236}Pu	1 787.9	1 788.6	1 787.1	1 787.4	1 788.2	1 788.5
^{238}Pu	1 800.9	1 801.1	1 799.7	1 800.5	1 800.9	1 801.4
^{240}Pu	1 813.2	1 813.7	1 811.6	1 812.6	1 813.2	1 813.6
^{242}Pu	1 825.1	1 825.5	1 822.9	1 824.4	1 824.7	1 825.2
^{244}Pu	1 836.3	1 836.2	1 833.7	1 835.6	1 835.9	1 836.3
^{238}Cm	1 795.8	1 797.2	1 795.5	1 794.8	1 796.2	1 796.5
^{240}Cm	1 809.6	1 811.0	1 809.1	1 808.9	1 810.0	1 810.3
^{242}Cm	1 822.9	1 824.2	1 822.0	1 821.9	1 823.1	1 823.1
^{244}Cm	1 835.7	1 836.9	1 834.4	1 834.5	1 835.8	1 835.9
^{246}Cm	1 847.8	1 848.8	1 845.9	1 846.7	1 847.9	1 847.8
^{248}Cm	1 859.2	1 859.5	1 856.3	1 858.2	1 859.3	1 859.2
^{250}Cm	1 870.2	1 870.2	1 866.3	1 869.0	1 869.4	1 869.7
^{242}Cf	1 816.7	1 818.9	1 815.8	1 815.4	1 817.2	1 817.3
^{244}Cf	1 830.8	1 832.9	1 829.7	1 829.8	1 831.4	1 831.3
^{246}Cf	1 844.4	1 846.3	1 843.1	1 843.3	1 844.8	1 844.8
^{248}Cf	1 857.4	1 859.0	1 855.5	1 855.9	1 857.8	1 857.8
^{250}Cf	1 869.7	1 871.0	1 866.9	1 868.5	1 870.3	1 870.0
^{252}Cf	1 881.5	1 882.4	1 877.8	1 880.2	1 881.3	1 881.3
^{254}Cf	1 892.8	1 892.9	1 888.5	1 891.6	1 891.7	1 892.1
^{246}Fm	1 836.9	1 839.1	1 835.8	1 835.6	1 837.6	1 837.2
^{248}Fm	1 851.4	1 853.4	1 850.3	1 849.7	1 852.0	1 851.6
^{250}Fm	1 865.2	1 867.0	1 863.7	1 864.0	1 866.0	1 865.5
^{252}Fm	1 878.3	1 880.0	1 876.1	1 876.7	1 879.3	1 878.9
^{254}Fm	1 891.0	1 892.5	1 887.9	1 889.4	1 891.2	1 891.0
^{256}Fm	1 903.1	1 903.7	1 899.6	1 901.5	1 902.4	1 902.5
^{252}No	1 871.3	1 873.2	1 870.7	1 869.7	1 872.0	1 871.3
^{254}No	1 885.3	1 887.2	1 884.1	1 883.6	1 886.3	1 885.6
^{256}No	1 898.8	1 900.7	1 897.0	1 897.1	1 899.1	1 898.6
^{256}Rf	1 890.4	1 892.6	1 890.7	1 888.5	1 891.5	1 890.7
^{260}Sg	1 908.9	1 911.9	1 909.0	1 907.1	1 909.9	1 909.0
^{264}Hs	1 926.8	1 930.2	1 926.6	1 925.9	1 927.6	1 926.7

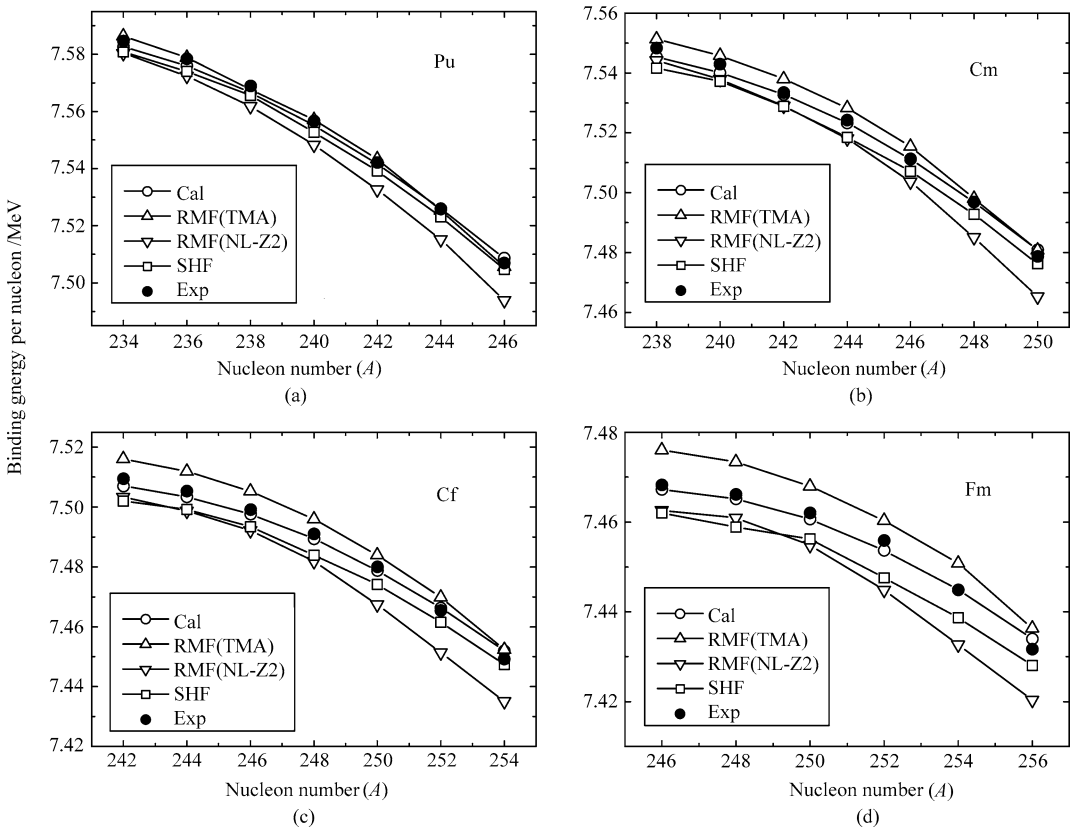

Fig. 2 Comparison of experimental binding energies (*dots*) [48] with theoretical ones from our calculation (*open circles*), from RMF model with TMA force (*open triangles*) and NL-Z2 force (*invert open triangles*) [25], and from SHF model (*open squares*) [29].

The results of rms deviations of binding energies and those of decay energies are listed in Table 9. One can see in Table 9 that all results of binding energies agree well with the experimental data because the rms deviations are very small as compared with the binding energies themselves. The precision of our MM calculation is as good as that of Möller's calculation as their rms deviations are very close. Because the rms deviations of the MM model (0.39 MeV and 0.23 MeV for binding energies and decay energies) are approximately equivalent to those of the Moller model (0.41 MeV and 0.26 MeV), it is concluded that their differences are very small and these small differences can be from the differences of the effective potentials in them. This shows that the MM model is reliable and stable when it is used in the superheavy region. The precision of the MM model is slightly better than that of SHF model and RMF model. At present it is not easy to say which model is the best with limited data of superheavy nuclei. The reason behind the good agreement is also to be explored with accumulation of more and more data. We may say that the MM results are slightly better for available data. In self-consistent mean-field models such as the RMF model the number of standard parameters is less than that of the MM model and Möller model. The MM model carefully treats the whole calculation as two steps. One is the macroscopic part and the other is the microscopic part. All of these could be the cause of differences of different models. We would like to say that all models work well in this range. The better agreement of one model with available data do not imply that other models are worse. We believe different models have different merits and different drawbacks. To explore the common merits of various models and to cure the common drawbacks of models are still open problems because current data will only be a part of the whole data of the superheavy region.

3.2 α-decay energy and half-life in ground state

α- decay energy is one of the most important properties of nuclei. From α-decay energy, we can get much information about the nuclear structure. For superheavy nuclei, the α-decay energy plays a key role because it is often used to identify new elements and new nuclides. In this section, we first concentrate on the α-decay energies of even-even nuclei with proton number $Z \leqslant 108$. Comparisons between the two sets of theoretical results and the experimental data are also made. For the heavier isotopes with proton number Z >108, we give a discussion on the new experimental data of recently synthesized superheavy nuclei.

Theoretical α-decay energy can be calculated by the binding energy difference of parent nucleus and daughter nucleus. In Table 2–6, the calculated α-decay energies are listed in column 5. Column 7 is for those of Möller's [30].

Experimental data are listed in the last column. From Table 2-6, we find that our results are very close to the experimental ones. The maximum difference is less than 0.7 MeV, and the average difference is approximately 0.3 MeV. Therefore our calculations reproduce well the measured values. The calculated α-decay energies are in good agreement with those of Möller's calculations also. This good agreement with experimental data and with Möller's results reconfirms the reliability of MM model. Our predicted α-decay energies for some unknown nuclei can be reliably used for future research.

In Fig. 3, we plot the variation of α-decay energies with neutron number for Pu, Cm, Sg, and Hs isotopes. We denote our results by hollow triangle, Möller's results by inverted hollow triangle, and black points for experimental data or estimated value. The comparisons include all available experimental data. Figure 3(a) shows results for Pu and Cm isotopes. It is clearly seen that both two sets of theoretical results agree well with the experimental one. The two sets of theoretical results are very close to each other. For Sg and Hs isotopes, the black points denote the experimental and estimated values obtained from Ref. [48], where the experimental α-decay energies are specially pointed out by a black arrow. From Fig.3(b), we find that the agreement between theoretical data and experimental data (or estimated value) is also satisfactory for Sg and Hs isotopes. This satisfactory agreement of α-decay energy strongly confirm the reliability of our calculation.

There is a noticeable increase of α-decay energy beyond neutron number N=162 both in theoretical results and experimental ones in Fig. 3(b), which means that there may be a deformed subshell at N=162, and this is in agreement with the discussion of Refs [5, 24, 26, 32]. The deformed subshell at N=162 can be clearly seen in Fig. 4 also.

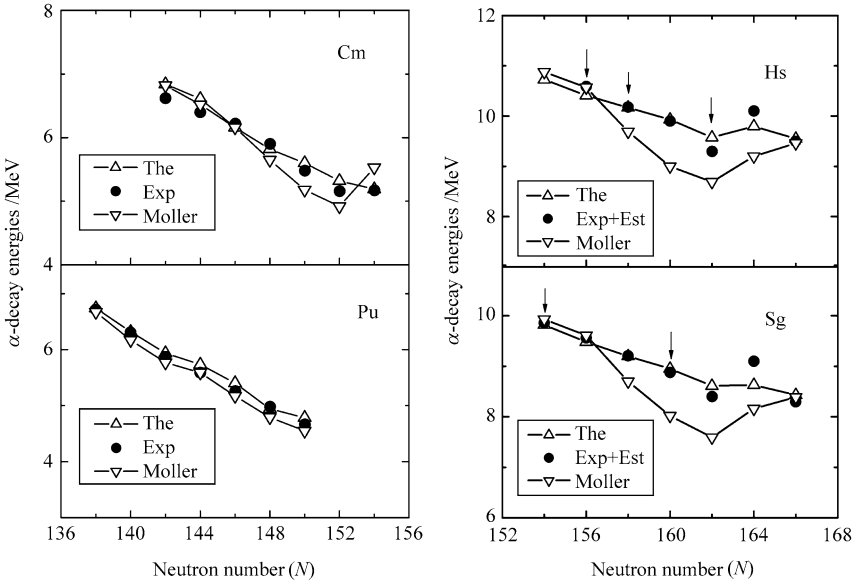

Fig. 3 The variation of α-decay energies of Pu, Cm, Sg and Hs isotopes with neutron number (N). The two sets of theoretical results are connected by solid curves. Möller's results [30] are denoted by inverted triangle. For Sg and Hs isotopes, the black points denote the experimental and estimated data obtained from the nuclear mass table of Audi [48], where the black points with a black arrow are experimental data. It is clearly seen from the figure that both theoretical results agree with the experimental data well.

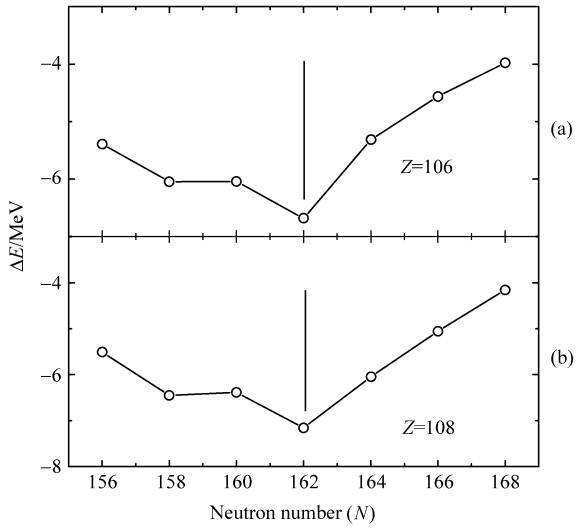

Fig. 4 Calculated shell correction energies for Sg, Hs, isotopes: (**a**) for isotopes of Sg; (**b**) for isotopes of Hs. The minimum in (a) and (b) is due to a large level spacing at N=162 for deformed nuclei. The minimum indicates that N=162 is a deformed subshell.

Compared with the experimental curve, our calculation slightly underestimates the subshell gap between N=162 and N=164 on the Q_α curve, but Möller's calculation slightly overestimates it [see Fig. 3(b)]. The reason for our slight underestimate may be the choice of κ and μ. Another reason may be the necessity for a more accurate treatment of pairing correction in the region of shell or subshell closure. If we choose these parameters and treat the pairing energy carefully, the results will be better.

In Table 8, we list calculated α-decay energies from our calculation, from RMF model [25], from SHF model [29] and from Möller's [30] calculation for isotopes with Z = 94–106. It is seen from Table 8 that our calculations provide slightly better α-decay energies. Figure 5 is the variation of different theoretical α-decay energies. It is clearly seen from the figure that our results are slightly closer to the experimental data, compared with results from other models. The rms deviation of α-decay energies for nuclei listed in Table 8 are calculated and listed in Table 9. The results show that our calculated α-decay energies have a slightly better precision. Although a little difference between rms of α-decay energies for different models, they are close to each other. From the comparison of rms deviation, we can conclude again that the MM model is reliable for α-decay energy and the results are insensitive to the choice of microscopic single-particle potential.

Since theoretical α-decay energy is in good agreement with experimental data, we expect good agreement with experimental α-decay half-life too. The Viola-Seaborg formula is usually used to estimate the half-life by the α-decay energies [24, 25, 31, 50]. Here we also use this formula to calculate the half-life according to theoretical α-decay energy [50]. Their expressions are given in the following.

$$\lg T_\alpha = (aZ+b)(Q_\alpha)^{-1/2} + (cZ+d) + h_{\log} \tag{16}$$

Table 8 The α-decay energies from our calculation, RMF [25], SHF [29], Möller *et al.* [30] and experiments [47].

Nuclei	The/MeV	TMA/MeV	Nl-Z2/MeV	SHF/MeV	Mol/MeV	Exp/MeV
^{234}Pu	6.32	5.48	5.50	6.21	6.17	6.31
^{236}Pu	5.87	5.16	5.18	5.91	5.77	5.87
^{238}Pu	5.62	4.72	4.98	5.51	5.59	5.59
^{240}Pu	5.40	4.45	4.83	5.71	5.17	5.26
^{242}Pu	4.94	4.05	4.25	5.41	4.79	4.98
^{244}Pu	4.78	4.47	3.95	5.11	4.55	4.67
^{238}Cm	6.84	6.25	6.55	7.32	6.82	6.62
^{240}Cm	6.61	5.83	6.34	6.82	6.52	6.40
^{242}Cm	6.16	5.49	6.04	6.92	6.16	6.21
^{244}Cm	5.75	5.09	5.50	6.42	5.65	5.90
^{246}Cm	5.65	5.41	5.36	6.02	5.18	5.48
^{248}Cm	5.49	5.00	5.65	5.72	4.92	5.16
^{250}Cm	5.10	4.52	5.49	5.42	5.53	5.17
^{242}Cf	7.39	6.64	8.02	7.72	7.33	7.52
^{244}Cf	7.09	6.40	7.73	7.42	6.90	7.33
^{246}Cf	6.84	6.24	7.23	6.92	6.50	6.86
^{248}Cf	6.65	6.26	7.18	6.82	6.27	6.36
^{250}Cf	6.37	5.73	7.30	6.52	5.87	6.13
^{252}Cf	5.99	5.34	6.89	6.22	6.25	6.22
^{254}Cf	5.70	5.55	6.09	5.72	6.00	5.93
^{246}Fm	8.05	8.07	8.25	8.12	7.82	8.37
^{248}Fm	7.76	7.80	7.72	8.32	7.64	8.00
^{250}Fm	7.55	7.61	7.71	7.62	7.19	7.56
^{252}Fm	7.34	7.20	7.74	7.52	6.79	7.15
^{254}Fm	6.98	6.80	7.27	7.42	7.39	7.31
^{256}Fm	6.71	7.00	6.45	7.02	7.24	7.03
^{252}No	8.32	8.57	7.86	8.32	8.35	8.55
^{254}No	8.14	8.11	7.82	8.72	7.97	8.27
^{256}No	7.84	7.68	7.38	7.92	8.57	8.58
^{256}Rf	9.26	8.85	8.26	9.52	8.75	8.93
^{260}Sg	9.82	9.08	10.02	9.72	9.93	9.92
^{266}Sg	8.95	8.57	8.67	9.32	8.02	8.66

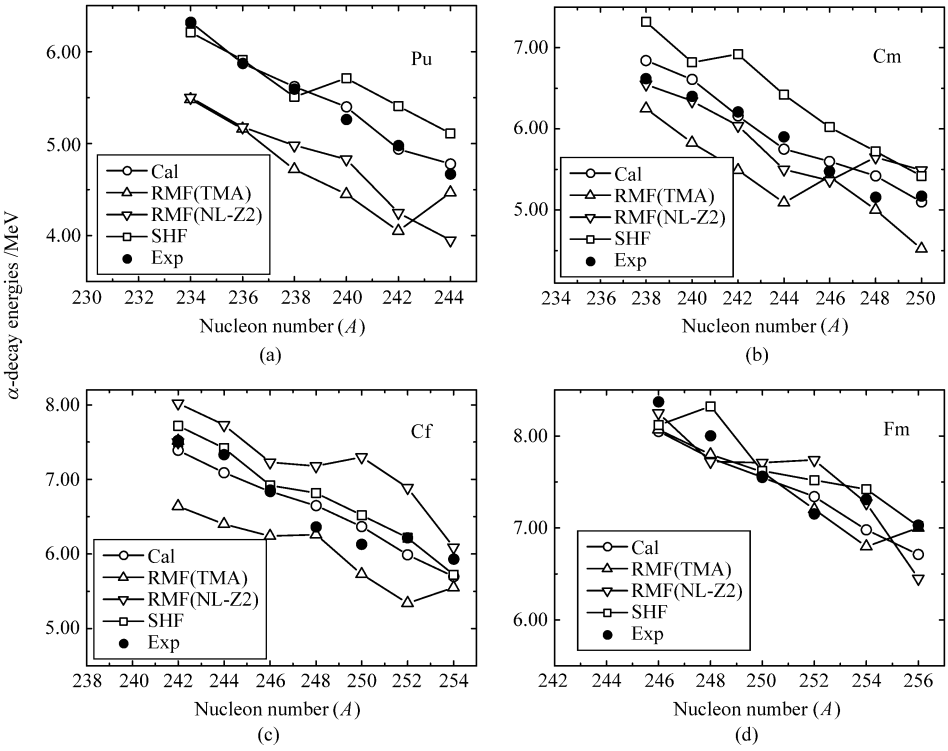

Fig.5 Comparison of experimental α-decay energies (*dots*) [48] with theoretical ones from our calculation (*open circles*), from RMF model with TMA force (*open triangles*) and NL-Z2 force (*invert open triangles*) [25], and from SHF model (*open squares*) [29].

Table 9 Comparison of rms deviations for binding energies and α-decay energies of different models. The calculated rms deviations of binding energies and α-decay energies are for nuclei listed in Table 7 and Table 8.

	The	TMA	Nl-Z2	SHF	Mol
Binding energy rms /MeV	0.391	1.402	2.045	1.415	0.414
α-decay energy rms /MeV	0.231	0.550	0.525	0.388	0.259

Table 10 Comparison of theoretical and experimental α-decay energies for recently synthesized superheavy nuclei.

Z	A	Q_α (The) /MeV	Q_α (Mol) /MeV	Q_α (Exp) /MeV	Ref.
118	294	12.12	12.28	11.81±0.06	[18]
116	292	11.07	10.82	10.80±0.07	[18]
	290	11.22	11.12	11.00±0.08	[18]
114	288	9.17	9.16	10.09±0.07	[18]
	286	9.99	9.39	10.35±0.06	[18]
112	284	9.80	8.69	9.35±0.05	[8]
	282	10.27	9.42	9.96±0.02	[48]
110	282	8.98	7.76	<10.82	[18]
	270	11.02	10.31	11.24±0.05	[15]
108	270	9.67	8.69	9.30±0.01	[48]
	266	10.17	9.69	10.38±0.02	[15]
	264	10.41	10.57	10.59±0.01	[48]

where T_α is given in seconds and Q_α in MeV, and Z is the proton number of the parent nucleus. The constants in this expression have been determined as a=1.66175, b = −8.516 6, c=−0.202 28, d =−33.906 9; $h_{\log}$=0.0 for even-even nuclei. These values are obtained by fitting the experimental data of medium and heavy nuclei.

Experimental half-life is taken from Audi *et al.* [48] and some new experimental data are from the publications in 2004 [17, 18]. Theoretical half-life is calculated according to the Viola-Seaborg formula. The numerical results of half-lives are plotted in Fig. 6. Both our theoretical results and Möller's results are plotted in this figure. Figure 6(a) is for Pu and Cm isotopes, and Fig. 6(b) is for Sg and Hs isotopes. From Fig.6(a), it is clear that for Pu and Cm isotopes, our theoretical results are in very good agreement with the experimental ones and with those of Möller's. The ratio between our theoretical half-lives and experimental

ones is less than 10^2 in many cases. Theoretical half-lives are quite good. One can also find that our calculations are in good agreement with Möller's calculations. From Fig. 6(b), we find that for Sg and Hs isotopes, theoretical half-lives still agree with experimental results and Möller's calculations. Although little difference exists between the two sets of theoretical results in this region, they agree with each other for global behavior.

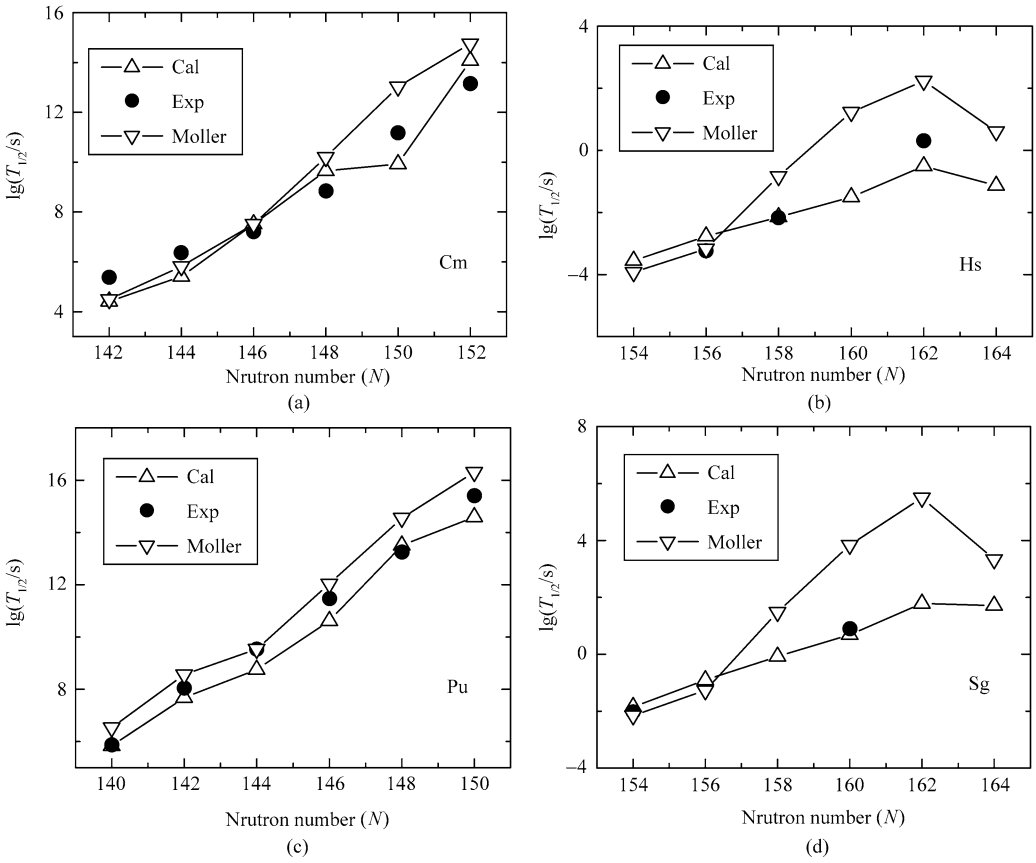

Fig. 6 The comparison of two sets of theoretical half-lives and experimental ones for Pu, Cm, Sg and Hs isotopes. Hollow triangle denotes our theoretical results, inverted triangle denotes the results of Möller's, and experimental data are represent by black points. The comparison includes all available ground-state half-lives of α -decays for these even-even nuclei on these isotopic chains. It is interesting to note that two sets of theoretical results are close to experimental data.

For isotopes with proton number Z >108, the experimental data are very few. But with recent experimental progress [4, 5, 16–18], some new experimental data the available now. These new data are useful for testing are reliability of different models. Here we tabulate the new synthesized experimental data in Table 9 and calculate. In the table, one can see that the agreement between theoretical results and experimental data is still acceptable, although there exists a slight difference. Therefore the MM model is also reliable in this region.

3.3 Deformations and shapes in the ground state of superheavy nuclei

It is well known that deformation plays an important role for the transuranium nuclei with proton number Z=92–102. Previous works suggest that the ground states of many nuclei have stable deformations [22–25, 30, 33, 42] and shape coexistence is important in superheavy nuclei [22–25, 28]. Here we investigate the shape, deformations and isomeric state for even-even superheavy nuclei in the framework of MM model.

In Table 2–6, we also tabulate the ground state quadrupole deformation and the hexadecapole deformation in columns 2–3. Now let us give a discussion on the deformations.For^{238,240,242,244}Pu, the deformations are known and the experimental values are approximately β_2 =0.29 [49]. The quadrupole deformations for above nuclei in our calculation are $\varepsilon_2 \approx 0.21$. They agree well with experimental data. Compared with other calculations, our results agree well with theoretical results [31, 42]. We can choose some data to demonstrate this . For ^{240}Pu, the deformations of Nilsson's calculation are ε_2 =0.20, ε_4 =−0.03 [42]. The values of our calculation are ε_2 =0.208,

ε_4 =−0.028, and therefore our calculation agrees well with Nilsson's calculation. The quadrupole deformation is ε_2 =0.208, ε_4 =−0.053 in Möller's calculation [31]. We can see that, even if we do not include the ε_6 deformation in our calculation, the quadrupole deformations are almost the same in the MM model but slightly different in hexadecapole deformation. The satisfying agreement of our results with Möller's theoretical results implies that the ε_6 deformation parameter has very little influence on the nuclear ground state properties. The satisfying agreement in deformations also confirms the reliability of our calculations again.

For Cm isotopes, the measured quadrupole deformation of ^{244,246,248}Cm is approximately $\beta_2 \approx 0.30$ [49]. They are close to our calculated results $\varepsilon_2 \approx 0.22$. The quadrupole deformation in Möller's calculation is $\varepsilon_2 \approx 0.217$ for above nuclei, which is also close to our results. Good agreement still holds true for Cm isotopes.

The comparison of other isotopes can also lead to the same conclusion, but we do not want to repeat it here. In short, the calculated deformations are in agreement with both measured values and other theoretical results. This shows that the theoretical deformations predicted by the MM model are acceptable.

From Table 2–6, one can see that the ground states of many superheavy nuclei have a stable quadrupole deformation around $\varepsilon_2 \approx 0.2$. This means that many of the superheavy nuclei are prolate deformed. However, it should be pointed out that in some cases an oblate shape may exist , such as ^{286}Hs, whose deformations are (−0.062,0.006) in our calculation and the deformations are (−0.075,0.020) in Möller's calculation. Both theoretical results predict that ^{286}Hs has an oblate shape. This is the shape coexistence in the ground state of the nuclei. Since the two sets of results are close, this means that, in the whole range, the calculations are satisfactory. Deformation plays an important role in superheavy nuclei and strongly affect their properties. The ground states of superheavy elements are considered to exhibit spherical shapes, prolate shapes, oblate shapes, and also coexistence of oblate and prolate shapes [23, 28]. Shape coexistence is interesting and important for the stability of superheavy nuclei. In the future, it would be interesting to study this problem in detail.

In Table 2–6, another noticeable trend is that for each isotopic chain the quadrupole deformation increases and then decreases with the increase of neutron number. This is a known behavior in medium and heavy nuclei. At the beginning of a new shell, there is prolate deformation, which increases with the increase of nucleon. After the middle of a shell, prolate deformation decreases and shape coexistence appears. In some case, the oblate deformation can be the ground state before shell closure.

In Fig. 7, we exhibit the total energy curve obtained for Cf, No, Sg and Z=114 as a function of quadrupole deformation parameter ε_2 where the energy is minimized with respect to ε_4 for each point. The general feature of this curve is in qualitative agreement with other theoretical calculations [23, 24, 42]. In Figs. 7(a)–(d), one can see that there are two minima in the energy curve. Because ground state should have the lowest energy, the lowest minimum of the curve is the ground state. It is clearly seen that there is a gradual transition from well-deformed nuclei with $\varepsilon_2 \approx 0.2$ to spherical shapes with the increase of proton number. For lighter nuclei (Z<108), the quadrupole deformation of nuclear ground state is about $\varepsilon_2 \approx 0.2$, and the nuclei of this region have prolate deformation. As the nucleon number increases, the quadrupole deformation has decreasing trend and gradually decreases to zero, which may indicate the appearance of a spherical shape.

Besides the two minima, we can also see there are two humps in the energy curve. The occurrence of the secondary minima ($\varepsilon_2 \approx 0.6$) corresponds to the isomeric state [51, 52]. It is seen from Fig. 7 that for Cf isotopes, nuclei around ^{244}Cf the shape isomeric state may exist. The same phenomena also exist in Pu and Cm isotopes. For No and Sg isotopes, the double hump fades away and the isomeric state disappears. But for nuclei around ^{286}114, the isomeric state seems to appear again. Isomeric state is important in superheavy nuclei because it affects the properties and stability of the superheavy nuclei. It is interesting and worth to studying in detail in the future.

From Fig. 7, one can find that the outer hump fades away for some transactinide nuclei with the increase of proton number, and this reconfirms the the earlier conclusion(see Ref. [42]). We find that the second hump will be slightly lower if we include the freedom of γ in our calculation. This means that the axial symmetry may be slightly broken when the nuclei have large deformation.

4 Conclusions

We have systematically calculated the ground state properties of even-even nuclei with proton number Z=94–118 by the macroscopic-microscopic model with the liquid drop model and with the modified single-particle oscillator potential. Our calculations have reproduced the experimental data quite accurately. The global agreement between the theoretical results and available experimental data is very impressive. The calculated binding energies are in good agreement with the available experimental data. For α-decay energy and half-life, the agreement between our numerical results and experimental data is still good. The calculations show that the ground states of many superheavy nuclei have prolate deformation ($\varepsilon_2 \approx 0.2$) and some of them have double humps in the energy curve. The outer hump gradually disappears with the increase of nucleon number for some isotopes, but it seems to appear again around the nucleus ^{286}114. The reliability of our calculation

is confirmed by the good agreement between theoretical results and experimental data.

A comparison is made between our calculation and that of Möller's. It is found that the ground state properties predicted by the two models agree well. The reliability of the MM model for superheavy nuclei is confirmed by the extensive comparison. We also compare calculated binding energies and α-decay energies with results from the RMF model and the SHF model. It is found that our results are close and slightly better than those of the RMF model and the SHF model. So the calculation here can be seen as an improvement with respect to previous results. This is a systematical calculation on superheavy nuclei based on the macroscopic liquid drop model and microscopic single-particle oscillator potential. It is also a detailed and complete comparison between theoretical results and experimental data. These comparisons are necessary to see the global behavior of the MM model and to test the reliability of the MM model. The results show that the MM model is insensitive to the microscopic single-particle potential. It is stable and can be reliably used as a theoretical model to study the structure and properties of superheavy nuclei.

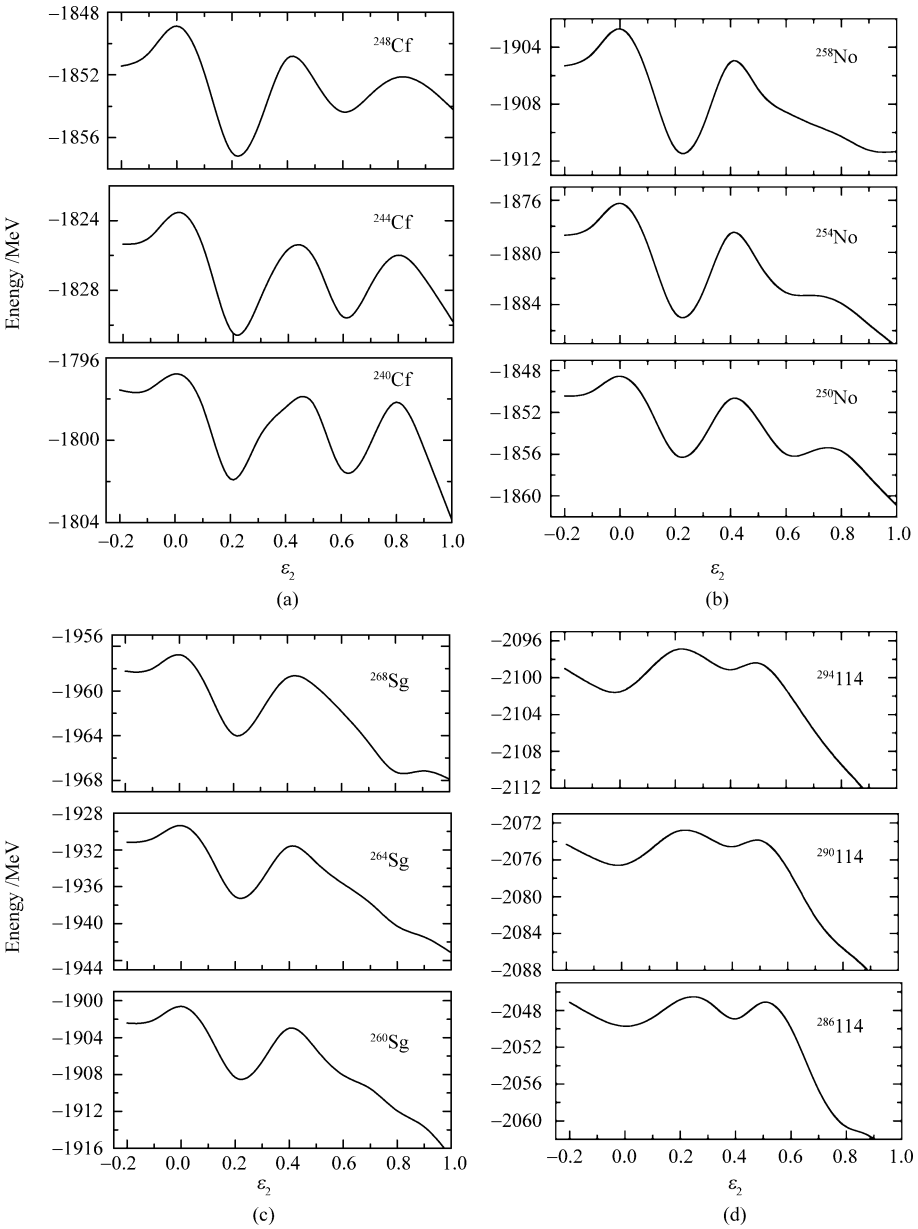

Fig. 7 The variation of the energies with quadrupole deformations for isotopes of Cf, No, Sg, and Z=114. The energies are minimized with respect to ε_4 for each ε_2, and the pairing strength is set independent with the nuclear surface area. It is clearly seen that the ground states of many nuclei are prolate deformed with $\varepsilon_2 \approx 0.2$. But in the vicinity of proton number Z=114, the ground state seems to have a spherically shape in the MM model.

Acknowledgements REN Zhong-zhou thanks Profs. SHEN W. -Q., ZHANG H. -Q., QIN Z., CAN Z. -G., GUO J. -S. for kindly communicating their new progress related to superheavy nuclei. This work is supported by the National Natural Science Foundation of China (Nos. 10125521, 10535010) and by the 973 National Major State Basic Research and Development of China (No. G2000077400).

1. S. Hofmann, V. Ninov, F.-P. Heβberger, P. Armbruster, H. Folger, G. Münzenberg, H.-J.Schött, A.-G. Popeko, A. -V. Yeremin, A.-N.

Andreyev, S. Saro, R. Janik and M. Leino, Z.Phys. A 350 ,1995:277
2. S. Hofmann, V. Ninov, F. -P. Heβberger, P. Armbruster, H. Folger, G. Münzenberg, H. -J.Schött, A. -G. Popeko, A. -V. Yeremin, A. -N. Andreyev, S. Saro, R. Janik and M. -S. Leino, Z.Phys. A 350 ,1995:281
3. S. Hofmann, V. Ninov, F.-P. Heβberger, P. Armbruster, H. Folger, G. Münzenberg, H. -J.Schött, A. -G. Popeko, A. -V. Yeremin, S. Saro, R. Janik and M. Leino, Z. Phys. A 354 ,1996:229
4. S. Hofmann, Rep. Prog. Phys., 1998, 61: 639
5. S. Hofmann, G. Münzenberg, Rev. Mod. Phys., 2000,72 : 733
6. Yu. -Ts. Oganessian, A.-V. Yeremin, A.-G. Popeko, S. -L. Bogomolov, G. -V. Buklanov, M. - L.Chelnokov, V. -I. Chepigin, B. -N. Gikal, V. -A. Gorshkov, G. -G. Gulbekian, M. -G. Itkis, A. -P. Kabachenko, A. -Y. Lavrentev, O. -N. Malyshev, J. Rohac, R. -N. Sagaidak, S. Hofmann, S.Saro, G. Giardina, and K. Morita, Nature ,1999,400:242
7. Yu. -Ts. Oganessian, V. -K. Utyonkov, Yu. V. Lobanov, F. Sh. Abdullin, A. -N. Polyakov, I. -V. Shirokovsky, Yu. S. Tsyganov, G.-G. Gulbekian, S.-L. Bogomolov, B.-N. Gikal, A. -N.Mezentsev, S. Iliev, V. -G. Subbotin, A. -M. Sukhov, G. -V. Buklanov, K. Subotic, and M. G.Itkis, Phys. Rev. Lett., 1999,83 : 3154
8. Yu. -Ts. Oganessian, V. -K. Utyonkov, Yu. -V. Lobanov, F. Sh. Abdullin, A. -N. Polyakov,I. -V. Shirokovsky, Yu. -S. Tsyganov, G.-G. Gulbekian, S.-L. Bogomolov, B.-N. Gikal, A. -N.Mezentsev, S. Iliev, V. -G. Subbotin, A. -M. Sukhov, O. -V. Ivanov, G. -V. Buklanov, K. Subotic,M. -G. Itkis, K. - J. Moody, J. -F. Wild, N. -J. Stoyer, M. -A. Stoyer, and R. -W. Lougheed, Phys.Rev. C 62 ,2000: 041604(R)
9. T. -N. Ginter, K. -E. Gregorich, W. Loveland, D. -M. Lee, U. -W. Kirbach, R. Sudowe, C. -M.Folden III, J. -B. Patin, N. Seward, P. -A. Wilk, P. -M. Zielinski, K. Aleklett, R. Eichler, H.Nitsche, and D. -C. Hoffman, Phys. Rev. C 67 ,2003:064609
10. K. Morita, K. Morimoto, D. Kaji, S. Goto, H. Haba, E. Ideguchi, R.Kanungo, K. Katori,H. Koura, H. Kuodo, T. Ohnishi, A. Ozawa, J. -C. Peter, T. Suda, K. Sueki, I. Tanihata, F.Tokanai, H. Xu, A. -V. Yeremin, A. Yoneda, A. Yoshida, Y.-L.Zhao, and T. Zheng, Nucl. Phys.A 734 ,2004:101
11. C.-M. Folden III, K. -E. Gregorich, Ch. -E. Düllmann, H. Mahmud, G. -K. Pang, J. -M. Schwantes,R. Sudowe, P. -M. Zielinski, H. Nitsche, D. -C. Hoffman, Phys. Rev. Lett., 2004,93 : 212702
12. Ch. -E. Düllmann, W. Brüchle, R. Dressler, K. Eberhardt, B. Eichler, R. Eichler, H. -W.Gäggeler, T. -N. Ginter, F. Glaus, K. -E. Gregorich, D. -C. Hoffman, E. JÄager, D. -T. Jost, U. -W. Kirbach,D. Piguet, Z. Qin, M. SchÄael, B. Schausten, E. Schimpf, H. -J. Schött, S. Soverna,R. Sudowe, P. Thörle, S. -N. Trautmann, A. Türler, A. Vahle, G. Wirth, A. -B. Yakushev, P. -M. Zielinski, Nature,2002, 418 :859
13. A. Türler, Ch. -E. Düllmann, H. -W. Gäggeler, U. -W. Kirbach, A. -B. Yakushev, M. Schädel, W. Brüchle, R. Dressler, K. Eberhardt, B. Eichler, R. Eichler, T. -N. Ginter, F. Glaus, K. -E.Gregorich, D. -C. Hoffman, E. Jäger, D. -T. Jost, D.M. Lee, H. Nitsche, J. -B. Patin, V. Pershina,D. Piguet, Z. Qin, B. Schausten, E. Schimpf, H.-J. Schött, S. Soverna, R. Sudowe, P. Thörle, S. -N. Timokhin, N. Trautmann, A. Vahle, G. Wirth and P. -M. Zielinski, Eur. Phys. J. A 17, 2003:505
14. Z. -G. Gan, J. -S. Guo, X. -L. Wu, Z. Qin, H. -M. Fan, X. -G. Lei, H. -Y. Liu, B. Guo, H. -G.Xu, R. -F. Chen, C. -F. Dong, F. -M. Zhang, H. -L. Wang, C. -Y. Xie, Z. -Q. Feng, Y,Zhen, L. -T. Song, P. Luo, H. -S. Xu, X. -H. Zhou, G. -M. Jin, and Zhongzhou Ren, Eur. Phys. J. A 20,2004:385
15. S. Hofmann, F. -P. Heβberger, D. Ackermann, S. Antalic, P. Cagarda, S. Cwiok, B. Kindler, J.Kojouharova, B. Lommel, R. Mann, G. Münzenberg, A. -G. Popeko, S. Saro, H. -J. Schött, A. -V.Yeremin, Eur. Phys. J. A 10,2001 :5
16. Yu. -Ts. Oganessian, V. -K. Utyonkov, Yu. -V. Lobanov, F. -Sh. Abdullin, A. -N. Polyakov,I. -V. Shirokovsky, Yu. -S. Tsyganov, G.-G. Gulbekian, S.-L. Bogomolov, B.-N. Gikal, A. -N.Mezentsev, S. Iliev, V. -G. Subbotin, A. -M. Sukhov, O. -V. Ivanov, G. -V. Buklanov, K. Subotic,M. -G. Itkis, K. -J. Moody, J. -F. Wild, N. -J. Stoyer, M. -A. Stoyer, R. -W. Lougheed, C. -A.Laue, Ye. -A. Karelin and A. -N. Tatarinov, Phys. Rev. C 63 ,2001: 011301(R)
17. Yu. -Ts. Oganessian, V. -K. Utyonkov, Yu. -V. Lobanov, F. -Sh. Abdullin, A. -N. Polyakov,I. -V. Shirokovsky, Yu. -S. Tsyganov, G. -G. Gulbekian, S. -L. Bogomolov, B. -N. Gikal, A. -N.Mezentsev, S. Iliev, V. -G. Subbotin, A. -M. Sukhov, A. -A. Voinov, G. -V. Buklanov, K. Subotic,V. -I. Zagrebaev, M. -G. Itkis, J. -B. Patin, K. -J. Moody, J. -F. Wild, M. -A. Stoyer, N. -J. Stoyer,D. -A. Shaughnessy, J. -M. Kenneally, and R. -W. Lougheed, Phys. Rev. C 69 ,2004: 054607
18. Yu. -Ts. Oganessian, V. -K. Utyonkov, Yu. -V. Lobanov, F. -Sh. Abdullin, A. -N. Polyakov,I. -V. Shirokovsky, Yu. -S. Tsyganov, G.-G. Gulbekian, S.-L. Bogomolov, B.-N. Gikal, A. -N.Mezentsev, S. Iliev, V. -G. Subbotin, A. -M. Sukhov, A. -A. Voinov, G. -V. Buklanov, K. Subotic,V. -I. Zagrebaev, M. -G. Itkis, J. -B. Patin, K. -J. Moody, J. -F. Wild, M. -A. Stoyer, N. -J. Stoyer,D.-A. Shaughnessy, J.-M. Kenneally, and R.-W. Lougheed, Phys. Rev. C 70 ,2004: 064609
19. W. -Q. Shen, J. Albinski, A. Gobbi, S. Gralla, K.-D. Hildenbrand, N. Herrmann, J. Kuzminski,W. -F. -J. Müller, H. Stelzer, J. Töke, B. -B. Back, S. Bj ϕ rnholm and S. -P. Sorensen, Phys. Rev.C 36,1987: 115
20. H.-Q. Zhang, Nuclear Physics Review,1999,16:192 (in Chinese)
21. Zhongzhou Ren, Z. -Y. Zhu, Y. -H. Cai, G. -O. Xu, J. Phys. G 22 ,1996: 1739
22. Zhongzhou Ren and H. Toki, Nucl. Phys. A 689 ,2001:691
23. Zhongzhou Ren, Phys. Rev. C 65 ,2002: 051304(R)
24. Zhongzhou Ren, D. -H. Chen, F. Tai, H. -Y. Zhang, and W. -Q. Shen, Phys. Rev. C 67 ,2003:064302
25. Zhongzhou Ren, F. Tai, and D. -H. Chen, Phys. Rev. C 66,2002: 064306
26. S. Cwiok, J. Dobaczewski, P.-H. Heenen, P. Magierski, and W. Nazarewicz, Nucl. Phys. A611,1996: 211
27. S. Cwiok, W. Nazarewicz, and P. -H. Heenen, Phys. Rev. Lett. ,1999,83 :1108
28. S. Cwiok, P. -H. Heenen, amd W. Nazarewicz, Nature,2005, 433: 705
29. S. Goriely, F. Tondeur, amd J. -M. Pearson, Ato. Dat. and Nucl. Dat. Tab., 2001,77: 311
30. P. Möller, J. -R. Nix, and K. -L. Kratz, Ato. Dat. and Nucl. Dat. Tab., 1997,66: 131
31. P. Möller, J. -R. Nix, K. -L. Kratz, W. -D. Myers, W. J. Swiatecki, Ato. Dat. and Nucl. Dat.Tab., 1995,59:185
32. P. Möller and J. -R. Nix, J. Phys. G 20 ,1994 : 1681
33. W. -D. Myers, and W. -J. Swiatecki, Ark. Phys. ,1967,36 :343
34. W. -D. Myers, and W. -J. Swiatecki, Phys. Rev. C 58 ,1998:3668
35. D. Lunney, J. -M. Pearson, C. Thibault, Rev. Mod. Phys., 2003,62 :1021
36. C. Andreoiu, T. D ϕ ssing, C. Fahlander, I. Ragnarsson, D. Rudolph, S. Åberg, R. -A. -E. Austin,M. -P. Carpenter, R. - M. Clark, R. -V. -F. Janssens, T. -L. Khoo, F. -G. Kondev, T. Lauritsen,T. Rodinger, D. -G. Sarantites, D. Seweryniak, T. Steinhardt, C. -E. Svensson, -O. Thelen, andJ. C. Waddington, Phy. Rev. Lett.,2003, 91 : 252502
37. A. -O. Evans, E. -S. Paul, J. Simpson, M. -A. Riley, D. -E. Appelbe, D. -B. Campbell, P. -T.W. Choy, R. -M. Clark, M. Cromaz, P. Fallon, A. Görgen, D. -T. Joss, I. -Y. Lee, A. -O.Macchiavelli, P. -J. Nolan, A. Pipidis, D. Ward, I. Ragnarsson, and F. Saric, Phy. Rev. Lett.,2004,92: 252502
38. T. Bengtsson, I. Ragnarsson, and S. Åberg, Phy. Lett. B 208 ,1988:39
39. I. Ragnarrson, Physica. Scripta 29 ,1984:385

40. K. Pomorski and J. Dudek. Phys. Rev. C 67 ,2003:044316
41. T. Bengtsson and I. Ragnarrson, Nucl. Phys. A 436 ,1985: 14
42. S. -G. Nilsson et al., Nucl. Phys. A 131,1969: 1
43. V. -M. Strutinsky. Nucl. Phys. A 95 ,1967:420
44. V. -M. Strutinsky. Nucl. Phys. A 122 ,1968: 1
45. J.-Y. Zhang, N. Xu, D. -B. Fossan, Y. Liang, R. Ma, and E. -S. Paul, Phys. Rev. C 39 ,1989:714
46. T. Bengtsson. Nucl. Phys. A 512,1990: 124
47. G. Audi, O. Bersillonb, J. Blachotb and A. -H. Wapstra, Nucl. Phys. A 729,2003: 3
48. G. Audi, A. -H. Wapstra, and C. Thibault, Nucl. Phys. A 729 ,2003: 337
49. S. Raman et al., Ato. Dat. and Nucl. Dat. Tab.,1987, 36: 1
50. V. -E. Viola Jr. and G. -T. Seaborg, J. Inorg. Nucl. Chem. ,1966,28: 741
51. H. -J. Specht, Rev. Mod. Phys. ,1974,46: 773
52. S. Bj ϕ rnholm and J. -E. Lynn, Rev. Mod.phys.1980,52:725